

Nano-Welding by Scanning Probe Microscope

Xiaojie Duan, Jin Zhang,* Xing Ling, and Zhongfan Liu*

Centre for Nanoscale Science and Technology, Key Laboratory for the Physics and Chemistry of Nanodevices, College of Chemistry and Molecular Engineering, Peking University, Beijing 100871, P.R. China

Received March 1, 2005; E-mail: jinzhang@pku.edu.cn; zfliu@pku.edu.cn

This paper reports on a procedure analogous to spot welding at the nanoscale level (nano-welding) using scanning probe microscopy (SPM). The nano-welding procedure was developed to immobilize single-walled carbon nanotubes (SWNTs) to the surface at point sites along their lengths. By SPM nano-welding and manipulation of SWNTs, bended, stretched, and more complex, such as triangle-like and wavelike, SWNTs have been obtained. It provides a versatile method for investigating SWNTs' deformation properties and fabricating SWNT-based nanodevices. Figure 1

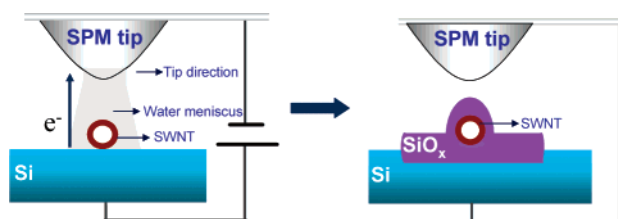


Figure 1. Schematic representation of the nano-welding by scanning probe microscope.

illustrates the mechanism of nano-welding (or nano-spot-welding) formation. Using a typical setup for conductive AFM oxidation, a positive bias voltage was introduced from the silicon substrate to the conductive SPM tip. When this occurred, the localized electric field induced oxidation of silicon to SiO_x . Because SiO_x is of much lower density than Si, the oxidation resulted in a volume expansion.^{1a,b} When performed over a SWNT, the SiO_x grew around the tube, effectively fixing that site on the SWNT to the silicon substrate.

In the past few years, many nanofabrication techniques have been developed that have greatly expanded our ability to construct a wide range of devices on the nanoscale.² Many of these are analogous to macroscale processes. Dip-pen³ and nanoimprint⁴ lithography, for example, correspond to writing and printing processes. For nanoscale construction, manipulation of structural morphology and configuration is often necessary.⁵ As one kind of nanofabrication, the nano-welding using SPM reported here represents a novel general means of manipulating nanostructures such as SWNTs that have a variety of applications.⁶

The carbon nanotubes used in this work were grown directly on silicon (111) surfaces by chemical vapor deposition as described in ref 7. Briefly, $\text{Fe}(\text{OH})_3$ colloid hydrolyzed from FeCl_3 was spin-coated onto silicon surface and then annealed in air at 400 °C for 20 min to generate ferric oxide nanoparticle catalysts. The growth was carried out at 900 °C for 10 min with a flow of methane at 600 standard cubic centimeter per minute (sccm). The diameter distribution of SWNTs showed a peak centered at 1.6 nm conforming to Raman spectroscopy.⁷ The nano-welding process and later manipulation were carried at Nanoscope III SPM (Veeco) using homemade software (see Supporting Information for details).^{8a,b} For a typical nano-welding process, the tip was brought down to the substrate by decreasing the setpoint while the feedback was held

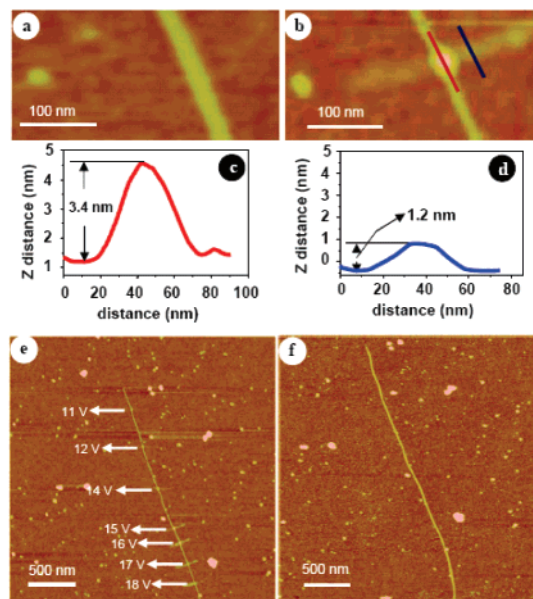


Figure 2. Tapping-mode AFM height images of a SWNT with a diameter of 1.8 nm before (a) and after (b) nano-welding. Panels c and d are the section analysis of (b) along the red line and blue line, respectively. (e) Tapping-mode AFM height images of a SWNT nano-welded using different voltages. Panel f shows the tapping-mode AFM height images of the same SWNT in (e) after SiO_x removal by NH_4F etching followed by annealing in air at 480 °C for 20 min.

on. After that, the voltage was added and the tip moved along a predefined path across the SWNT. The voltage employed in our experiment was in a range of 10–18 V, and the tip moving speed was 10 nm/s except in those cases indicated. The relative humidity was in a range of 30–50%. As for the manipulation, the process was similar, except that the voltage was set at zero; the feedback was switched off, and the tip was additionally pressed down about 10 nm for an optimal contact load at the tip–sample interface.

Figure 2a,b shows the AFM height images of a SWNT before and after the welding. The height increase at the welding spot suggested that scanning probe oxidation of the Si had deposited SiO_x above and around SWNTs, which could be completely removed by fluoride etching for the SWNT to return to its original height, as shown in Figure 2e,f (see S1 in the Supporting Information for more evidences for the formation of capping SiO_x). Most importantly, the section analysis indicates that the SiO_x on SWNTs (3.4 nm) was much thicker than that at the area without SWNTs (1.2 nm), and this is essential for the fixing. The reasons for this enhancement may be that the presence of a SWNT had changed and increased local electric field distribution at the SWNT site.^{9,10} Similar to the welding in the macroscopic world, the strength of this nano-welding may be modulated by changing the bias voltage, oxidation time (Supporting Information, Figure S2), or the humidity.¹⁰

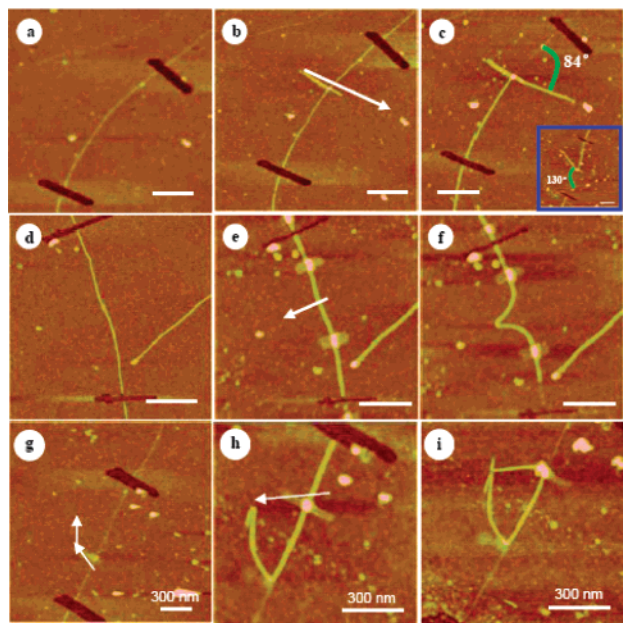


Figure 3. Tapping-mode AFM height images of a bending (a–c) and stretching (d–f) process using SPM nano-welding and manipulation. Inset of (c) is a bended SWNT with a controlled angle of 130° . Panels g–i show the process of fabricating the triangle-like SWNT. More detailed description is available in the text. Scale bar in a–f is 500 nm. The spotty line left behind the original position of the SWNT may be the contamination from amorphous carbon.

For exploring the properties of SWNTs and the construction of nanodevices, it was necessary to establish whether the SWNT had sustained any damage during nano-welding. To do this, SWNTs were welded at various bias voltages from 11 to 18 V and a tip speed of 10 nm/s to cover all the conditions used in our nano-welding experiments (Figure 2e). After removing the SiO_x by NH_4F etching and annealing the SWNT in air at 480°C for 20 min, they were examined by AFM. Annealing in this way is an effective means of revealing defect sites since fracture usually occurs as a result of the annealing process.^{11a,b} Not only were no fractures seen but also no obvious morphological changes were observed. This result suggested that nano-welding did not alter the SWNT structure and excluded the possibility of forming carbide at welding spots.

This nano-welding technique, together with SPM manipulation,¹² will help us to deform SWNTs in a controlled manner to produce structures with unique properties predicted both experimentally¹³ and theoretically.¹⁴ In Figure 3a–c, the SWNT was first welded at a predefined point and then manipulated along the white arrow. Due to the nano-welding, the SWNT took up a bended configuration. It can be seen that the bending site and angle can be easily controlled through predefining the tip path. In the case of Figure 3c, the angle is 84° , while for the tube shown in the inset, the angle is controlled at 130° . The nano-welding can also be used to stretch the SWNT. As shown in Figure 3d–f, after the SWNT was welded at two sites, the manipulation was carried out between the two welded sites along the white arrow. Due to the presence of the nano-welding, the SWNT has been elongated about 2% as shown in panel f. It should be noticed that due to the extraordinary strength of SWNTs,¹⁵ the force imposed by the welding seems to be unable to survive the large stress resulting from the stretch. So the SWNT has a slide under the SiO_x accompanying the elongation. This can be seen from the movement of the nether end of the SWNT. One of the appealing advantages of this welding is that the welding can

be conducted during the manipulation process. This is useful for the construction of more complex SWNT-based structures. In Figure 3 g–i, through a second nano-welding and manipulation, a triangle-like SWNT-based structure was fabricated. Another example is shown in Figure S3 of the Supporting Information, where a wavelike SWNT has been obtained by repeating the welding and manipulation processes.

In summary, a procedure analogous to spot welding at the nanoscale level, termed nano-welding, using SPM is presented in this communication. Using SPM oxidation of the underlying silicon, SWNTs have been immobilized to the surface at point sites along their lengths. It is shown that this nano-welding process nearly has no structural damage to the SWNTs, and this immobilization makes the SPM manipulation of SWNTs controllable and desirable, which is helpful not only for the construction of SWNT-based nanodevices but also for the exploration of the SWNTs' properties, including the mechanical properties. The idea of using SPM for welding at the nanoscale may be amenable to other nanofabrication technologies and other systems, such as DNA.¹⁶ This highly novel nano-welding technique will permit the development of a whole range of new nanodevices and facilitate exploration of material physics at the nanometer scale.

Acknowledgment. This work was supported by the National Natural Science Foundation of China (NSFC 90206023), Ministry of Science and Technology of China (2001CB6105), and FOKY-TUNG Education Foundation (94012). We are grateful to Prof. C. Robinson (University of LEEDS, UK) for his kind help and useful discussion.

Supporting Information Available: Part I: Method of nano-welding and manipulation by SPM; Part II: Figure S1, AFM images of the welding point before and after destruction; Figure S2, AFM images of SWNTs nano-welded with different voltages and tip moving speeds; Figure S3, AFM images of intermediate stages of the process to fabricate the wavelike SWNT. This material is available free of charge via the Internet at <http://pubs.acs.org>.

References

- (1) (a) Nyffenegger, R. M.; Penner, R. M. *Chem. Rev.* **1997**, *97*, 1195. (b) Wouters, D.; Schubert, U. S. *Angew. Chem., Int. Ed.* **2004**, *43*, 2480.
- (2) Chen, Y.; Pepin, A. *Electrophoresis* **2001**, *22*, 187.
- (3) Piner, R. D.; Zhu, J.; Xu, F.; Hong, S.; Mirkin, C. A. *Science* **1999**, *283*, 661.
- (4) Chou, S. Y.; Krauss, P. R.; Renstrom, P. J. *J. Vac. Sci. Technol.* **1996**, *14*, 4129.
- (5) Postma, H. W. C.; Teepen, T.; Yao, Z.; Grifoni, M.; Dekker, C. *Science* **2001**, *293*, 76.
- (6) Popov, V. N. *Mater. Sci. Eng. Rep.* **2004**, *43*, 61.
- (7) He, M. S.; Duan, X. J.; Wang, X.; Zhang, J.; Liu, Z. F.; Robinson, C. J. *Phys. Chem. B* **2004**, *108*, 12665.
- (8) (a) Ling, X.; Zhu, X.; Zhang, J.; Zhu, T.; Liu, M. H.; Tong, L. M.; Liu, Z. F. *J. Phys. Chem. B* **2005**, *109*, 2657. (b) Li, Q. G.; Zheng, J. W.; Liu, Z. F. *Langmuir* **2003**, *19*, 166.
- (9) Zheng, L. F.; Li, S. D.; Brody, J. P.; Burke, P. J. *Langmuir* **2004**, *20*, 8612.
- (10) Avouris, P.; Hertel, T.; Martel, R. *Appl. Phys. Lett.* **1997**, *71*, 285.
- (11) (a) Li, Q. W.; Yan, H.; Ye, Y. C.; Zhang, J.; Liu, Z. F. *J. Phys. Chem. B* **2002**, *106*, 11085. (b) Data not shown that fracture has happened under this annealing condition, where there was no welding, and it may come from the defect formed in the growth process.
- (12) Hertel, T.; Martel, R.; Avouris, P. *J. Phys. Chem. B* **1998**, *102*, 910.
- (13) Liu, L.; Jayanthi, C. S.; Tang, M. J.; Wu, S. Y.; Tomblar, T. W.; Zhou, C. W.; Alexseyev, L.; Kong, J.; Dai, H. *J. Phys. Rev. Lett.* **2000**, *84*, 4950.
- (14) Liu, L.; Jayanthi, C. S.; Wu, S. Y. *Phys. Rev. B* **2001**, *64*, 033412.
- (15) Qian, D.; Wagner, G. J.; Liu, W. K.; Yu, M. F.; Ruoff, R. S. *Appl. Mech. Rev.* **2002**, *55*, 495.
- (16) Severin, N.; Barner, J.; Kalachev, A. A.; Rabe, J. P. *Nano Lett.* **2004**, *4*, 577.

JA051280R